

1 **HYDRA2 – A Multispectral Data Analysis Toolkit for sensors on Suomi**

2 **NPP and other current satellite platforms**

3

4 Tom Rink, W. Paul Menzel, Liam Gumley, and Kathy Strabala

5

6 Space Science and Engineering Center

7 Madison, Wisconsin, 53706 USA

8

9 (from the BAMS 2016 publication by the same name)

10 **Abstract**

11

12 The HYper-spectral data viewer for Development of Research Applications version 2  
13 (HYDRA2) is a freeware-based multispectral analysis toolkit for satellite data that assists  
14 scientists in research and development as well as education and training of remote  
15 sensing applications. HYDRA2 users can explore and visualize relationships between  
16 sensor measurements (brightness temperatures for infrared and reflectances for  
17 visible/near infrared wavelengths) using spectral diagrams, cross sections, scatter plots,  
18 multi-band combinations, and color enhancements on a pixel by pixel basis.

19

20 HYDRA2 can be used with direct broadcast and archived data from sensors onboard the  
21 NOAA/NASA Suomi National Polar-orbiting Partnership (S-NPP), NASA Aqua/Terra,  
22 EUMETSAT MetOp, and Chinese Feng Yun-3 platforms.

23

24 This paper describes HYDRA2 and presents some examples using data retrievals from

25 the S-NPP Visible Infrared Imaging Radiometer Suite (VIIRS), Cross-track Infrared  
26 Sounder (CrIS), Advanced Technology Microwave Sounder (ATMS), as well as  
27 Terra/Aqua Moderate resolution Imaging Spectro-radiometer (MODIS) instruments.

28

## 29 **1. Overview of HYDRA2**

30

31 HYDRA2 (Hyper-spectral data viewer for Development of Research Applications  
32 version 2) is an update to the capabilities of HYDRA (Rink et al., 2007). The “HYDRA”  
33 concept is based on over 10 years of continued development of interactive satellite data  
34 interrogation and visualization tools offered at the University of Wisconsin’s (UW) Space  
35 Science and Engineering Center (SSEC) remote sensing workshop series  
36 (<http://cimss.ssec.wisc.edu/rss/>) and direct broadcast seminars  
37 (<http://cimss.ssec.wisc.edu/dbs/>). The salient requirements for HYDRA2 remain similar  
38 to those of its predecessor: it must be (a) freely available to the global community, (b)  
39 computer platform independent, and (c) extendable. Essentially, HYDRA2 is a stand-  
40 alone app based on the VisAD (Visualization for Algorithm Development, Hibbard et al.,  
41 2002) Java library to integrate data from various satellite sensors, ground based  
42 instruments, and forecast models into very interactive, high performance, 2D/3D  
43 displays.

44

45 A primary motivation of this new effort is to support the Suomi National Polar orbiting  
46 Partnership (S-NPP) and the upcoming Joint Polar Satellite System (JPSS) missions, as  
47 well as maintaining existing support for the MODIS sensors onboard the Terra and Aqua  
48 platforms.. To achieve this, HYDRA2’s custom VisAD data adapters for cross-track

49 polar swath were improved to have greater flexibility and a more clearly defined  
50 programmatic interface. These improvements also facilitated the transitioning of datasets  
51 onboard the MetOp and FengYun (FY) satellite series into HYDRA2 with only a modest  
52 level of effort.

53

54 HYDRA2 enables the user to inspect multispectral (broad band and hyperspectral) fields  
55 of data so that (a) spectral measurements can be easily displayed at pixel locations; (b)  
56 colors can be assigned to pixel values and false color images can be viewed; (c) images  
57 of spectral band combinations can be constructed; (d) scatter plots can be determined  
58 from imagery containing individual or combined spectral bands; individual pixel values  
59 can be obtained either from scatter plots or imagery; (e) transects of measurements from  
60 imagery can be displayed, and (f) measured spectra and the derived temperature and  
61 moisture profiles from individual pixels can be displayed and studied.

62

63 Many improvements in the user interface and analysis tools have been implemented in  
64 HYDRA2 based on ongoing user feedback. These include: (1) linking the zooming,  
65 roaming, and interrogation between multiple image display windows, (2) combining  
66 spectral bands or linear combinations of spectral bands from multiple sensors (e.g.,  
67 MODIS and VIIRS) onto a single image display, (3) managing datasets in a consistent  
68 manner, (4) eliminating VIIRS and MODIS cross-track scan “bowtie” artifacts in the re-  
69 gridding process, (5) aggregating consecutive and separate file granules into a single  
70 cohesive image, and (6) enabling image display export to KML/KMZ for transport to  
71 Google™ Earth.

72

73 The evolution from HYDRA to HYDRA2 has been motivated, in part, by rapid  
74 advancements in software development technology over the last decade. HYDRA2  
75 consists of a higher functioning Java class-only application compared to the slower  
76 performing Jython scripting language used in HYDRA. Perhaps more importantly, the  
77 software components that comprise HYDRA2 have been generalized so that any scripting  
78 language that supports Java (e.g. Jython or JRuby) can be used to develop, for example, a  
79 user-defined computation interface. HYDRA2 employs the Java-NetCDF library, which  
80 is the Java implementation of Unidata's CDM (Common Data Model), for access to  
81 HDF4/5 format data which is currently used in MODIS and several S-NPP instruments.  
82 The Java-NetCDF library merges the storage data models of many file formats, including,  
83 but not limited, to NetCDF3/4, GRIB1/2 and WMO BUFR, to create a common  
84 application program interface (API) for many types of scientific data including multi-  
85 dimensional arrays. This updated version effectively provides computer platform and  
86 storage format independent access from a single library.

87

88 HYDRA2 uses the NetBeans© IDE (Integrated Development Environment) from  
89 Oracle®, which improves the processing efficiency of more robust source code  
90 development. HYDRA2 is deployed with platform-specific point and click installers  
91 generated by Install4j© from EJ-Technologies. The YourKit Java profiler is employed to  
92 reduce any excessive and wasteful allocation of CPU memory during runtime.. Source  
93 code revision management is handled within a GitHub repository via Git integration in  
94 NetBeans©. Unlike HYDRA, HYDRA2 is entirely self-contained within the installer,  
95 i.e., no additional libraries are needed. Graphics card drivers still require upgrades,  
96 when necessary.

97

98 The following sections provide some examples of HYDRA2 analyzing data from S-NPP  
99 that include VIIRS, CrIS, and ATMS – see eoPortal  
100 <https://directory.eoportal.org/web/eoportal/satellite-missions/s/suomi-npp>.

101 HYDRA2 is also capable of viewing and interrogating data from the Terra and Aqua  
102 platform sensors that includes MODIS and the Atmospheric Infrared Sounder (AIRS) –  
103 see eoPortals <https://directory.eoportal.org/web/eoportal/satellite-missions/a/aqua> and  
104 <https://directory.eoportal.org/web/eoportal/satellite-missions/t/terra>. In addition, data  
105 from the MetOp (Klaes et al. 2007) Infrared Atmospheric Sounding Interferometer  
106 (IASI), Advanced Very High Resolution Radiometer (AVHRR), High resolution Infrared  
107 Radiation Sounder (HIRS), and Microwave Humidity Sounder (MHS) can also be  
108 displayed – see eoPortal [https://directory.eoportal.org/web/eoportal/satellite-](https://directory.eoportal.org/web/eoportal/satellite-missions/m/MetOp)  
109 [missions/m/MetOp](https://directory.eoportal.org/web/eoportal/satellite-missions/m/MetOp). And recently, data from the FY-3 (see  
110 <https://directory.eoportal.org/web/eoportal/satellite-missions/pag-filter/-/article/fy-3>)  
111 Medium Resolution Spectral Imager (MERSI) was also added to the HYDRA2  
112 capabilities.

113

## 114 **2. Examples of Spectral Band Applications with HYDRA2**

115

116 Expanding on the capabilities of HYDRA, HYDRA2 enables display and interrogation of  
117 the available spectral bands (22 for VIIRS and 36 for MODIS) for any pixel within a  
118 granule of data. Reflectance or brightness temperatures can be displayed for individual  
119 pixels within the granule. Red-green-blue (RGB) composites using any combination of  
120 single and/or multiple spectral bands can be created. Transects from one location to

121 another can be constructed for a given spectral band to determine a variety of remote  
122 sensing characteristics, e.g., min/max values, pattern matching (clouds vs other features),  
123 gradients, etc.

124

125 Figure 1 shows the VIIRS infrared window I5 (11.45  $\mu\text{m}$ ) brightness temperature image  
126 of the eye of Typhoon Vongfong from 7 October 2012 in false color (with red colder and  
127 blue warmer in an inverse rainbow color enhancement). The high spatial resolution (375  
128 m) of VIIRS shows the eyewall structure in excellent detail. Using HYDRA2  
129 commands, brightness temperature for each spectral band with corresponding locations  
130 (latitudes/longitudes) for each pixel can be displayed.

131

132 Figure 2 demonstrates the transect capability of HYDRA2. A transect is superimposed  
133 on the VIIRS infrared window M15 (10.8  $\mu\text{m}$ ) image and the associated brightness  
134 temperature values are plotted from west to east along a 1500 km line centered on the eye  
135 of Typhoon Vongfong; brightness temperatures range from 190 K (cold, clouds near the  
136 eye) to 290 K (clear skies in the eye and further away over warm ocean surfaces).

137

138 Differences of spectral bands are often useful in highlighting atmospheric or surface  
139 features. In Figure 3, a VIIRS-derived split window image was created using Band Math  
140 (IR window M15 at 10.8  $\mu\text{m}$  minus the water vapor sensitive IR window M16 at 12.0  
141  $\mu\text{m}$ ); the brightness temperature difference is sensitive to atmospheric moisture with  
142 larger differences usually indicating more moisture. The highest clouds associated with  
143 the typhoon on the southwest perimeter are readily apparent because of the dryness above  
144 the clouds (indicated by differences of less than 1 K).

145

146 The VIIRS Day-Night Band (DNB, centered at  $0.7 \mu\text{m}$ ) is shown in Figure 4 capturing  
147 the night-time illumination over a segment of the Korean peninsula on 26 August 2012 at  
148 1619 UTC; the stark contrast between the brightly reflective industrialized regions  
149 covering South Korea versus the unlit dark environment over North Korea is readily  
150 evident. In addition, fishing activity is also noticeable within the open water region to the  
151 east and southeast of South Korea. The DNB offers a new dimension of imaging  
152 capability, that of low light visible reflectances at night. Miller et al. (2012) provide  
153 more details on the new remote sensing opportunities offered by the VIIRS DNB.

154

155 HYDRA2 has the capability to compare measurements between any two sensors. Figure  
156 5 shows a comparison of the brightness temperatures measured by MODIS (band 31,  
157  $11.0 \mu\text{m}$ ) in the lower left and the VIIRS high resolution imager (band I5,  $11.5 \mu\text{m}$ ) in the  
158 lower right on 30 August 2012 over the southern portion of South Korea, the island of  
159 Jeju-do, and the open waters nearby. The overpass times are separated by less than 20  
160 minutes. The higher spatial resolution of the VIIRS measurements ( $0.375 \text{ km}$ ) reveals  
161 sharper details than MODIS ( $1 \text{ km}$  at nadir) across the coastline; this is evident in the  
162 annotated transect where the corresponding brightness temperature plot reveals a more  
163 detailed VIIRS profile (shown in magenta) versus the smoother MODIS profile (shown in  
164 green). The finer detail provided by VIIRS is most apparent away from nadir; VIIRS  
165 nadir resolution is constrained to grow by a factor of 2 across the entire swath, while the  
166 MODIS pixel size grows unconstrained to roughly 6 times by the edge of a narrower  
167 swath. In summary, HYDRA enables detailed comparisons of measurements between  
168 different sensors in transects, overlays, and scatter plots.

169

170 Figure 6 shows a scatter plot of visible (0.55  $\mu\text{m}$ ) reflectances plotted on the y-axis  
171 against infrared window (10.8  $\mu\text{m}$ ) brightness temperatures on the x-axis. Different  
172 colors highlight pixels in the scatter plot that are associated with regions circled in the  
173 visible reflectance image (purple shows cold and reflecting cloud pixels, green warm and  
174 non-reflecting vegetated surfaces, and blue warm and non-reflecting ocean). When two  
175 HYDRA windows have been established (containing a spectral band image, or spectral  
176 band combination image, or a derived product image) a scatter plot of the values in both  
177 windows can be compared against each other. In the scatter plot configuration, one can  
178 locate values either within the scatter plot or its corresponding imagery. Locating pixels  
179 in the scatter plot and associating them with pixels in the window display image as well  
180 as vice versa enables users to estimate threshold values for discriminating certain land,  
181 ocean, or atmospheric features.

182

183 Figure 7 shows the HYDRA2 display of the VIIRS DNB image over Columbia, South  
184 America on 30 January 2015 transferred to Google Earth mapping; this enables the  
185 colocation tools from Google Earth to be applied to the HYDRA2 data set. This example  
186 further demonstrates the ability to differentiate lightning versus city lights; west of the  
187 city lights around Medellin one finds illumination that cannot be associated with any city  
188 and is likely caused by cloud to cloud lightning.

189

190 HYDRA2 also has the capability to display several MODIS Level 2 Atmospheric product  
191 files; they include the following:

192



193 MOD04: Aerosol products  
194 MOD06: Cloud products  
195 (see Figure 8 for an example display of the MODIS cloud top pressure)  
196 MOD14: Thermal Anomalies - Fires and Biomass Burning  
197 MOD28: Sea Surface Temperature  
198 MOD35: Cloud Mask

199

200 Figure 8 shows the derived product image of the Aqua MODIS cloud top pressure  
201 associated with 30 August 2012 at 440 UTC; two cloud groups, the first at ~300 hPa and  
202 the second at ~800 hPa, are evident. HYDRA2 will incorporate the display of VIIRS  
203 Environmental Data Record (EDR) products in the near future.

204

### 205 **3. Hyperspectral and microwave data analysis with HYDRA2**

206

207 HYDRA2 can also be used to analyze granules of hyperspectral CrIS data in much the  
208 same way AIRS data were analyzed with HYDRA (Rink et al., 2007). Colocation in  
209 space and time is readily displayed with HYDRA2 for the VIIRS, CrIS, and ATMS  
210 sensors on S- NPP (as well as with MODIS and AIRS sensors on Terra and Aqua and the  
211 IASI sensors on MetOp). This section will demonstrate HYDRA2 analysis tools for  
212 viewing CrIS and ATMS data separately and together.

213

214 Figure 9 shows the HYDRA2 display of CrIS data over Typhoon Vongfong on 7 October  
215 2012. The top panel displays a spectrum measured by CrIS over a clear pixel well away  
216 from the typhoon center (shown in aqua) and another spectrum measured over clouds

217 near the eye of the typhoon (shown in black). The brightness temperature infrared  
218 window image at 902.25 cm<sup>-1</sup> (bottom panel) shows warm and cold regions. Within the  
219 spectrum plot, the clear brightness temperature spectrum (in black) shows the absorption  
220 of CO<sub>2</sub> at ~660 cm<sup>-1</sup>, O<sub>3</sub> at ~1050 cm<sup>-1</sup>, and H<sub>2</sub>O at ~1500 cm<sup>-1</sup> (causing notably  
221 cooler brightness temperatures in the positive lapse rate troposphere). The cloudy  
222 brightness temperature spectrum is remarkable for the near constant temperature  
223 regardless of wavenumber, indicating that the observed cloud is so high that above it  
224 there is very little H<sub>2</sub>O and only small amounts of CO<sub>2</sub> and O<sub>3</sub> (causing somewhat  
225 warmer brightness temperatures in the negative lapse rate stratosphere).

226

227 CrIS measurements (at roughly 15 km spatial resolution) are used to derive temperature  
228 and moisture profiles in clear skies and above clouds (portions of the atmosphere where  
229 the measurements of at least some of the CrIS spectral bands are not affected by clouds).  
230 Figure 10 shows the stratospheric temperatures at 96.1 hPa (above the typhoon) derived  
231 using a Dual Regression profile retrieval (Weisz et al., 2013) along with a sounding of air  
232 temperature along the vertical pressure axis above the clouds at a position (annotated by  
233 187.73 K) northwest of the typhoon and another position (annotated by 198 K) in the  
234 center of the eye. This remarkably well-formed eye, captured in a near perfect nadir view  
235 by CrIS on Suomi-NPP, reveals warm temperatures (290 to 300 K) for the lowest 400  
236 hPa in the troposphere.

237

238 ATMS measurements provide a sounding capability in clear and cloudy (non-  
239 precipitating) conditions, albeit at relatively coarse (~50 km) spatial resolution. Figure 11  
240 shows the image of ATMS brightness temperatures measured at 31.4 GHz (channel 2)

241 over Typhoon Vongfong coincident with the VIIRS and CrIS data (shown in Figure 10)  
242 along with brightness temperature spectra covering clear conditions (annotated by 262.56  
243 K) within the eye and cloudy features (annotated by 186.09 K) to the northwest of the  
244 eye. The absorption features in the spectrum caused by O<sub>2</sub> (centered on channel 10 at  
245 57.3 GHz) and H<sub>2</sub>O (centered on channel 18 at 183.3 GHz) are evident as colder  
246 temperatures within the clear eye region. An additional contribution to the radiation in  
247 the microwave spectrum is the reflection from the surface (especially the ocean) in the  
248 more transparent spectral channels.

249

250 Figure 12 shows a scatter plot of ATMS 31.4 GHz brightness temperatures (x-axis)  
251 versus CrIS derived temperatures retrieved for 96.1hPa (y-axis) over Typhoon Vongfong.  
252 Different colored boxes highlight pixels in the scatter plot that are shown in the CrIS  
253 retrieval image; the cold ATMS temperatures reveal a ring of clouds in the northwest  
254 quadrant of Typhoon Vongfong while the warm ATMS temperatures isolate the ring of  
255 clouds around the eye.

256

#### 257 **4. Summary**

258

259 HYDRA2 enables users from a variety of educational backgrounds to explore and  
260 investigate satellite sensor measurements. Starting from HYDRA, HYDRA2 has been  
261 adapted to accommodate data from more sensors, including those on SNPP. HYDRA2  
262 has become a part of the Community Satellite Processing Package (CSPP) that can be  
263 found at <http://cimss.ssec.wisc.edu/cspp>. The HYDRA2 command structure and  
264 enhanced visualizations tools are described in more detail at:

265 <http://cimss.ssec.wisc.edu/cspp/download/>. Instructions for downloading this freeware  
266 are also provided within the website.

267

## 268 **Acknowledgements**

269

270 This paper relied on extensive user participation that consisted of many students and  
271 international colleagues in beta testing the HYDRA2 freeware. We thank them for their  
272 enthusiasm and useful feedback. Funding from the NASA IMAPP (International MODIS  
273 and AIRS Processing Package) and the NOAA CSPP (Community Satellite Processing  
274 Package) programs is also gratefully acknowledged.

275

## 276 **References**

277

278 Bill, R. W., 2002: *Jython for Java Programmers*. New Riders Publishing. ISBN 0-7357-  
279 1111-9. 465 pp.

280

281 Hibbard, W., and Coauthors, 2002: Java Distributed Objects for Numerical Visualization  
282 in VisAD. *Commun. ACM*, **45**, 160-170.

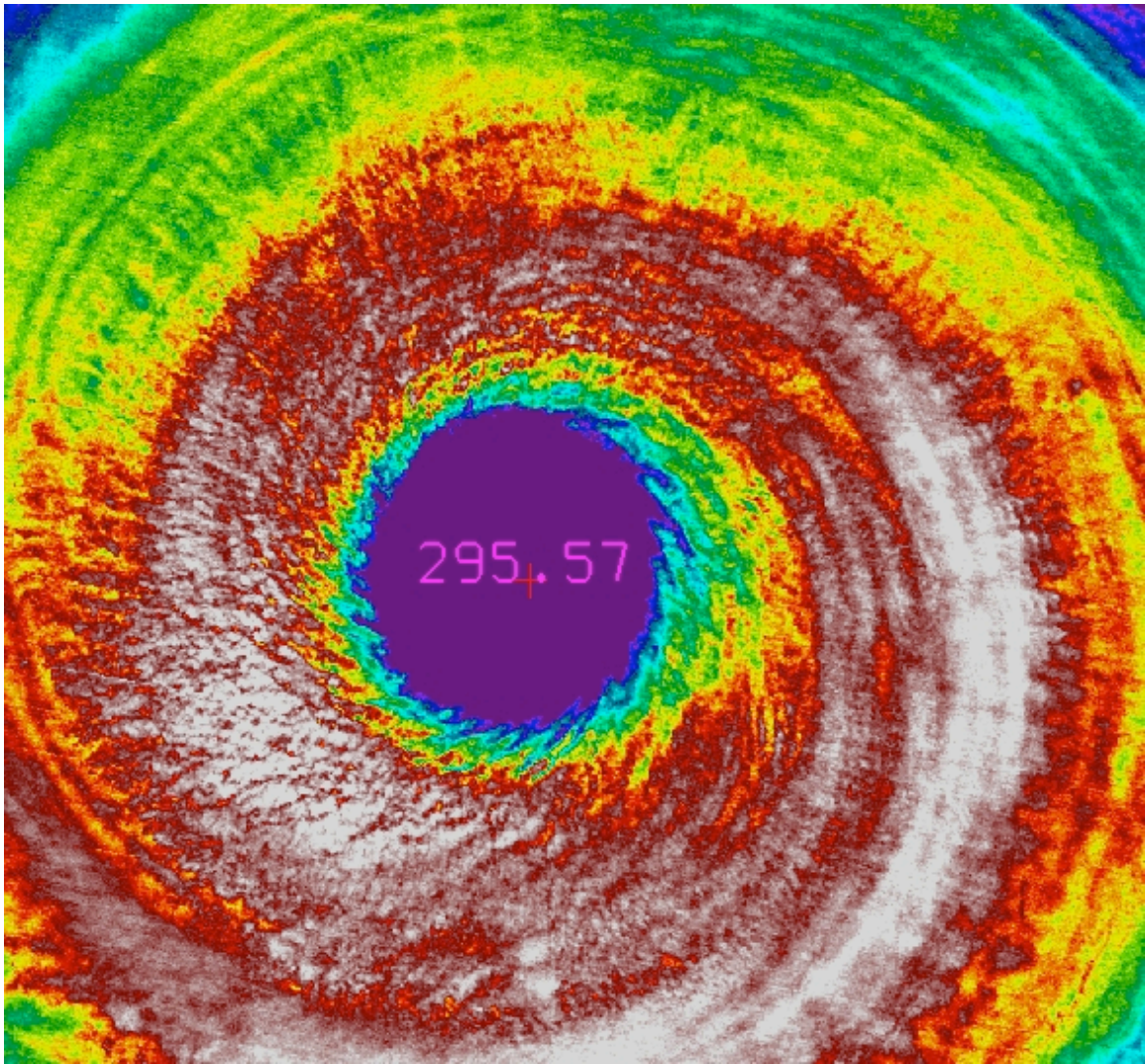
283

284 Klaes, K. D., and Coauthors, 2007: An introduction to the EUMETSAT polar system.  
285 *Bull. Amer. Meteor. Soc.*, **88**, 1085–1096.

286

287 Lutz, M., G. Rossum, L. Lewin, and F. Willison, 1996: *Programming Python*. USENIX.  
288 Mark Lutz Programming Python O'Reilly & Associates, 1996. ISBN 1-56592-

289           197-6. 880 pp.  
290  
291 Miller, S. D., S. P. Mills, C. D. Elvidge, D. T. Lindsey, T. F. Lee, and J. D. Hawkins,  
292           2012: Suomi satellite brings to light a unique frontier of environmental imaging  
293           capabilities. *Proc. Nat. Acad. Sci.*, **109**(39), 15706-15711.  
294  
295 Rink, T., W. P. Menzel, P. Antonelli, T. Whittaker, K. Baggett, L. Gumley, and A.  
296           Huang, 2007: Introducing HYDRA – a Multispectral Data Analysis Toolkit. *Bull.*  
297           *Amer. Meteor. Soc.*, **88**, 159-166.  
298  
299 Weisz, E., W. L. Smith, N. Smith, 2013: Advances in simultaneous atmospheric profile  
300           and cloud parameter regression based retrieval from high-spectral resolution  
301           radiance measurements. *J. Geophys. Res.-Atmospheres*, **118**, 6433-6443  
302



303

304

305 **Figure 1:** VIIRS infrared window image (I5, 11.5  $\mu\text{m}$ ) of the eye of Typhoon Vongfong

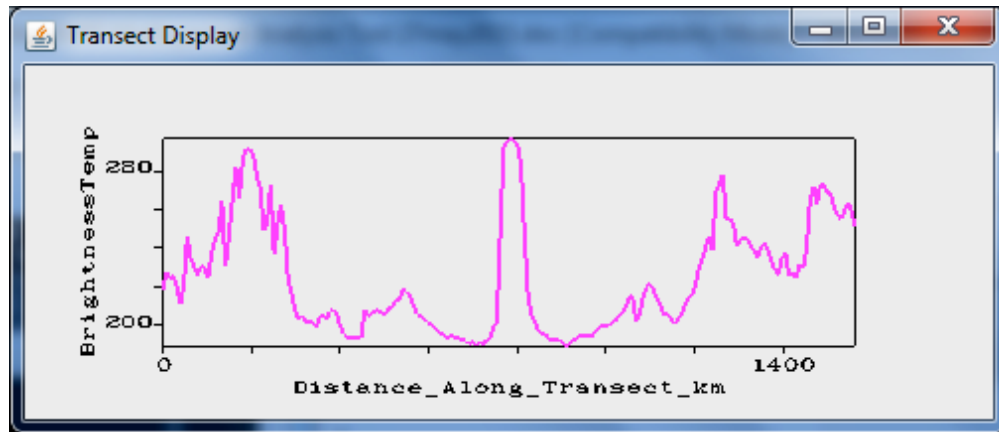
306 on 7 October 2014 with inverse rainbow color enhancement (reds start at 190 K, greens at

307 195 K, and blues end at 205 K). The brightness temperature in the eye of Typhoon

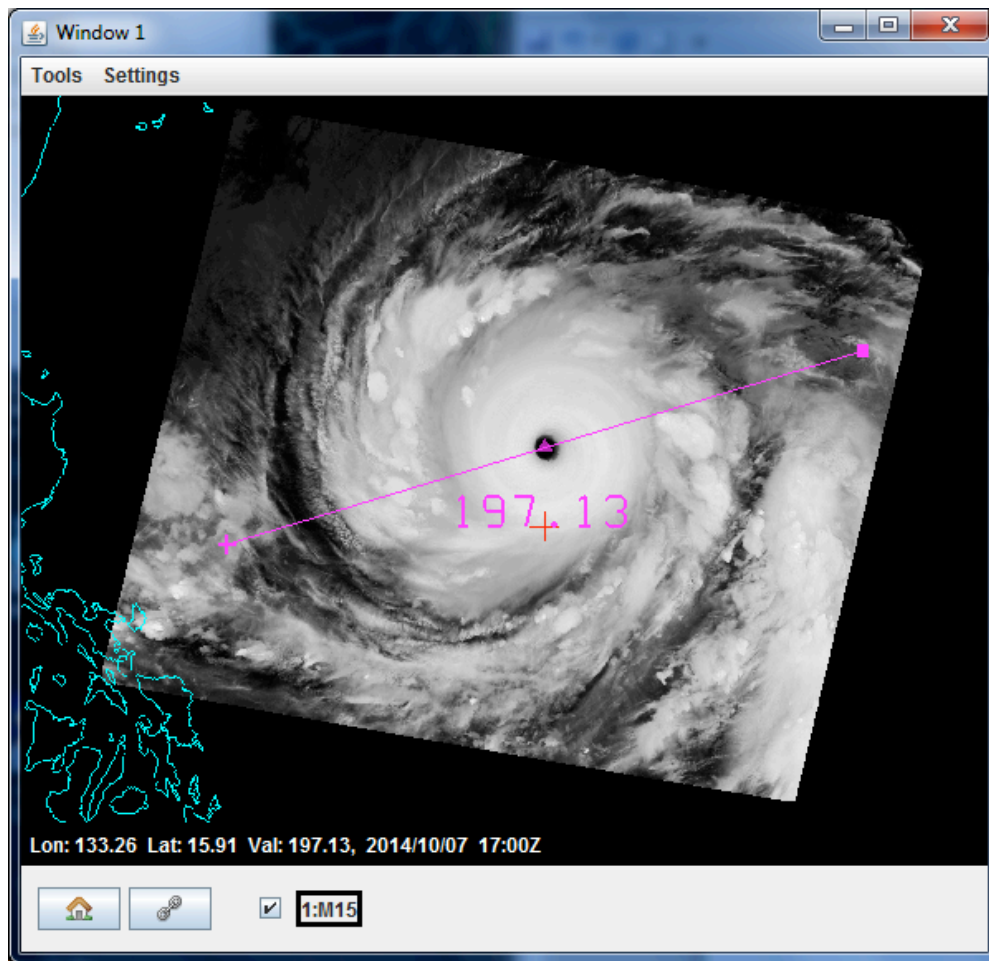
308 Vongfong is 295.6 K.

309

310

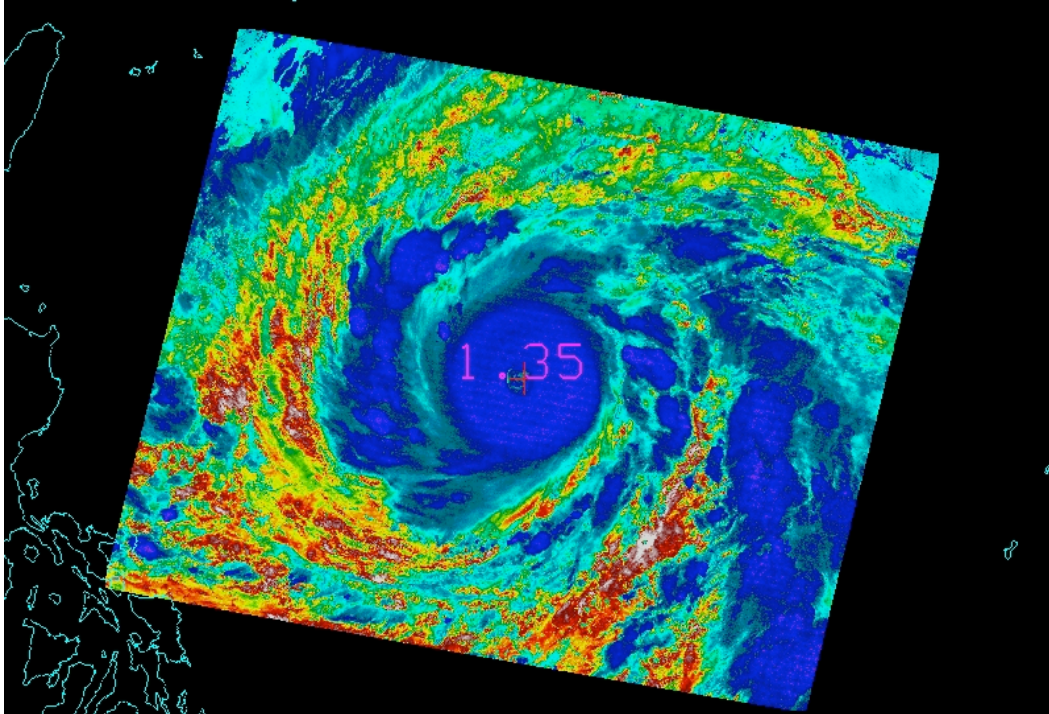


311

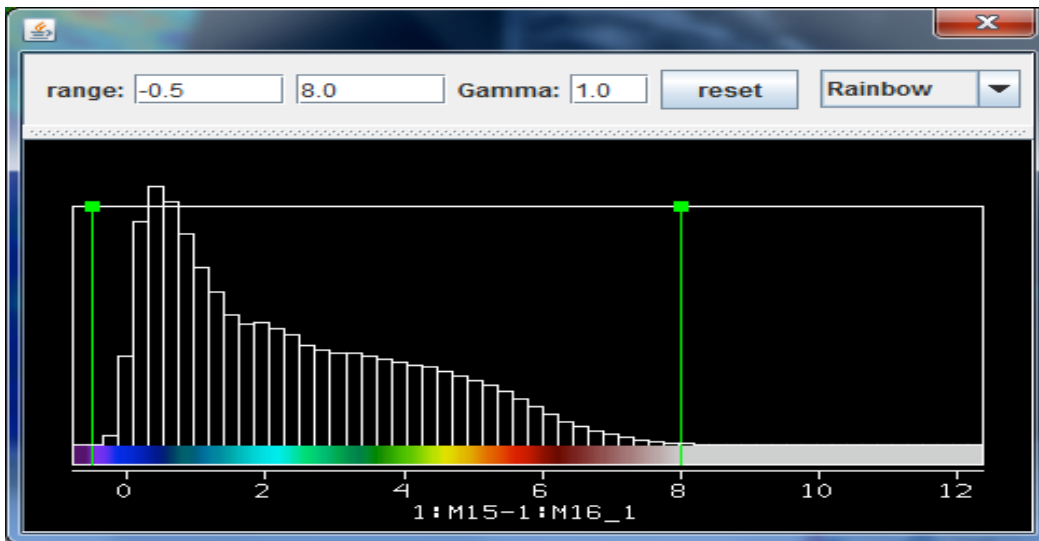


312

313 **Figure 2:** Infrared window brightness temperatures (top) in degrees Kelvin for the  
314 indicated transect in the 10.8  $\mu\text{m}$  brightness temperature M15 image (bottom) proceeding  
315 from left (west) to right (east). Distance along the transect is indicated in kilometers.



316

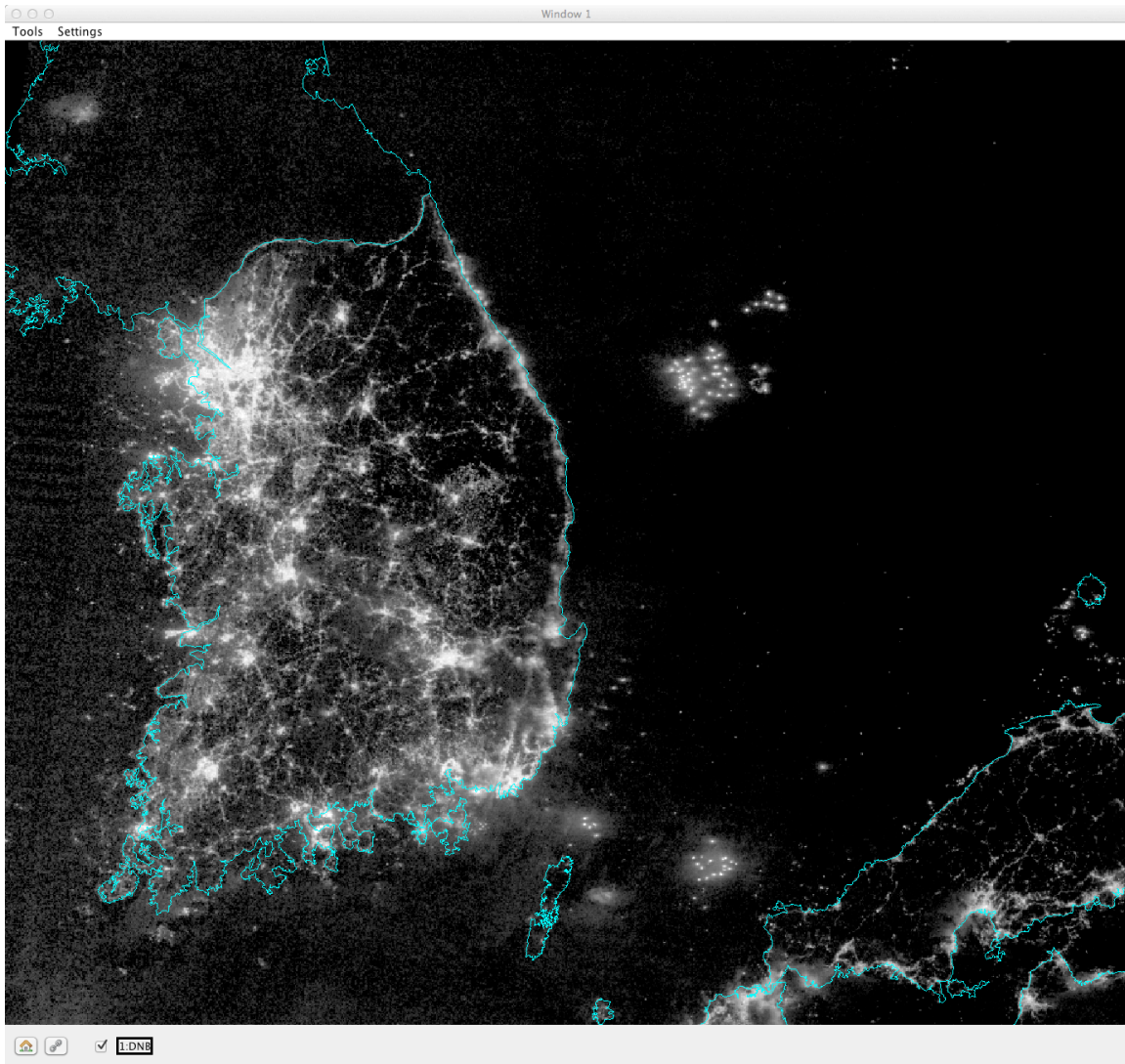


317

318

319 **Figure 3:** (top) False color image of brightness temperature difference (degrees K)  
 320 between the water vapor insensitive IR window (M15) and the water vapor sensitive IR  
 321 window (M16). (bottom) Color scale indicates the temperature difference along with  
 322 histogram distribution within the image. Higher amounts of atmospheric moisture will  
 323 produce larger differences; note the relative dryness above the high typhoon clouds.





324

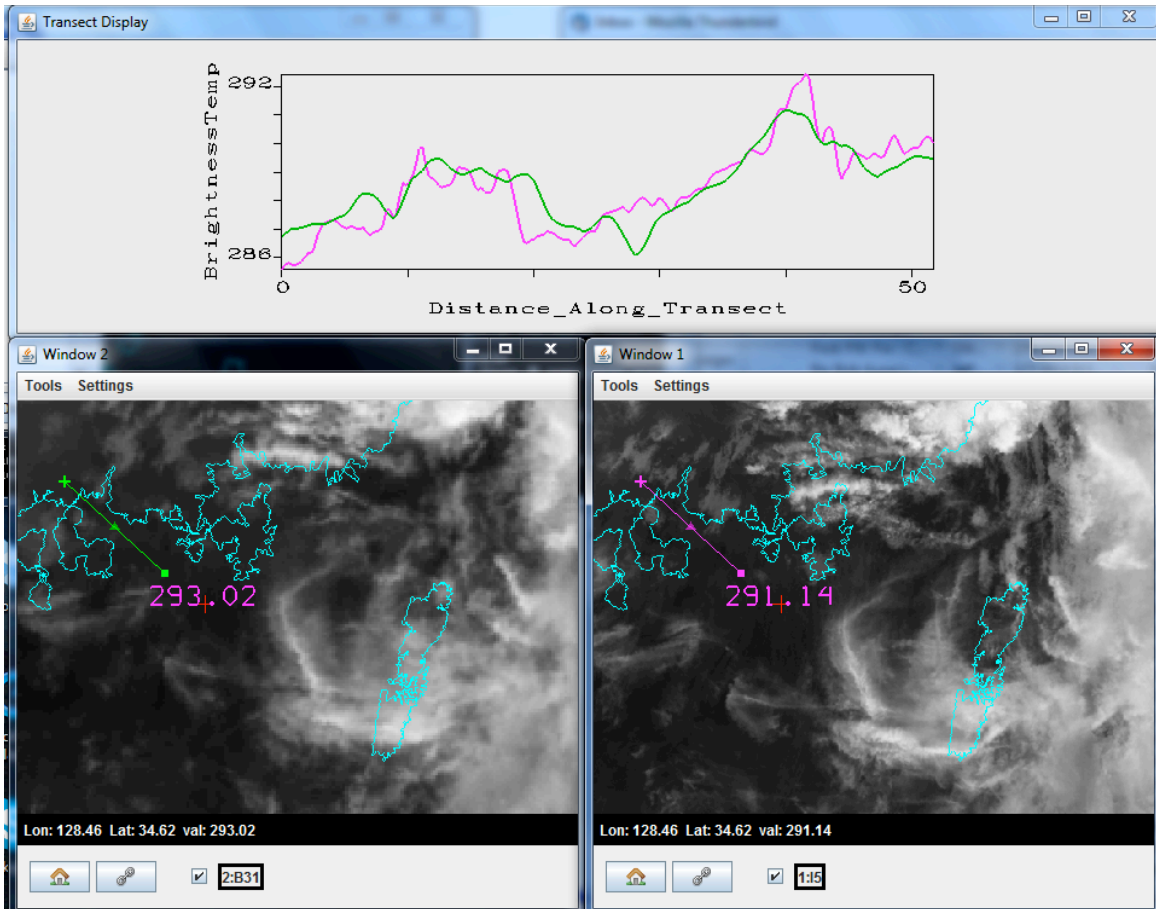
325

326 **Figure 4:** VIIRS DNB image of the Korean peninsula from 26 August 2012 at 1619

327 UTC. Lights from the cities and night time fishing are evident, as well as the stark

328 contrast in lighting between North and South Korea.

329



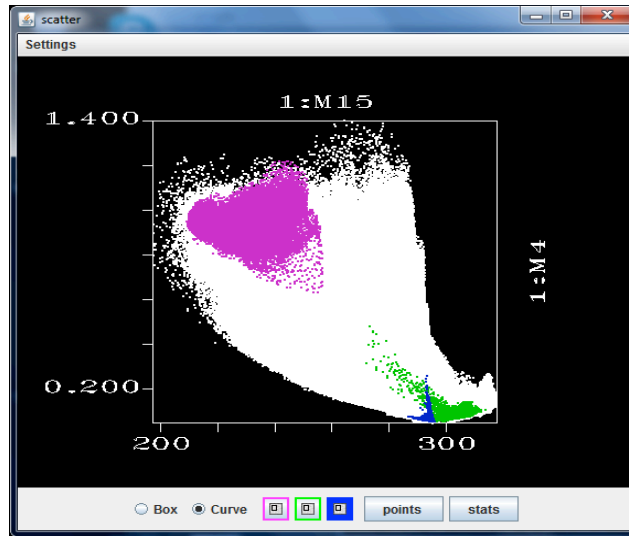
330

331

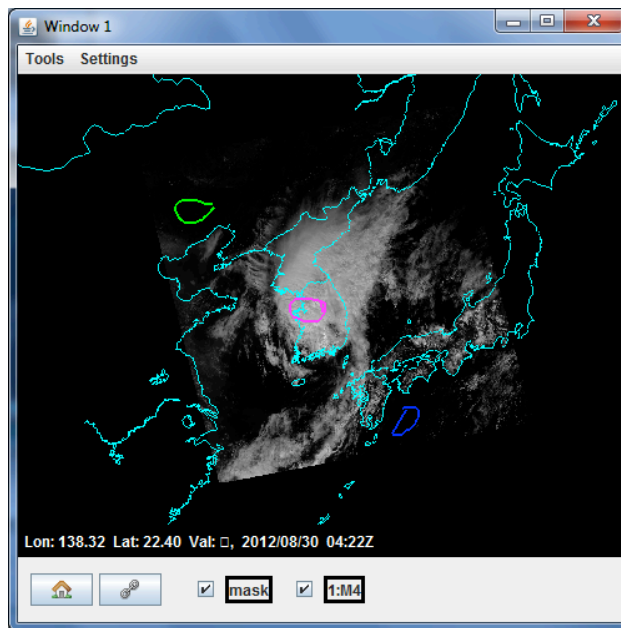
332 **Figure 5:** Comparison of 30 August 2012 VIIRS 11.5  $\mu\text{m}$  infrared window I5 at 375 m  
 333 nadir resolution (bottom right) from 422 UTC and corresponding MODIS 11.0  $\mu\text{m}$   
 334 infrared window Band 31 at 1 km nadir resolution from 440 UTC (bottom left) along  
 335 with a transect over clear skies (top). All units are in degrees Kelvin.

336

337

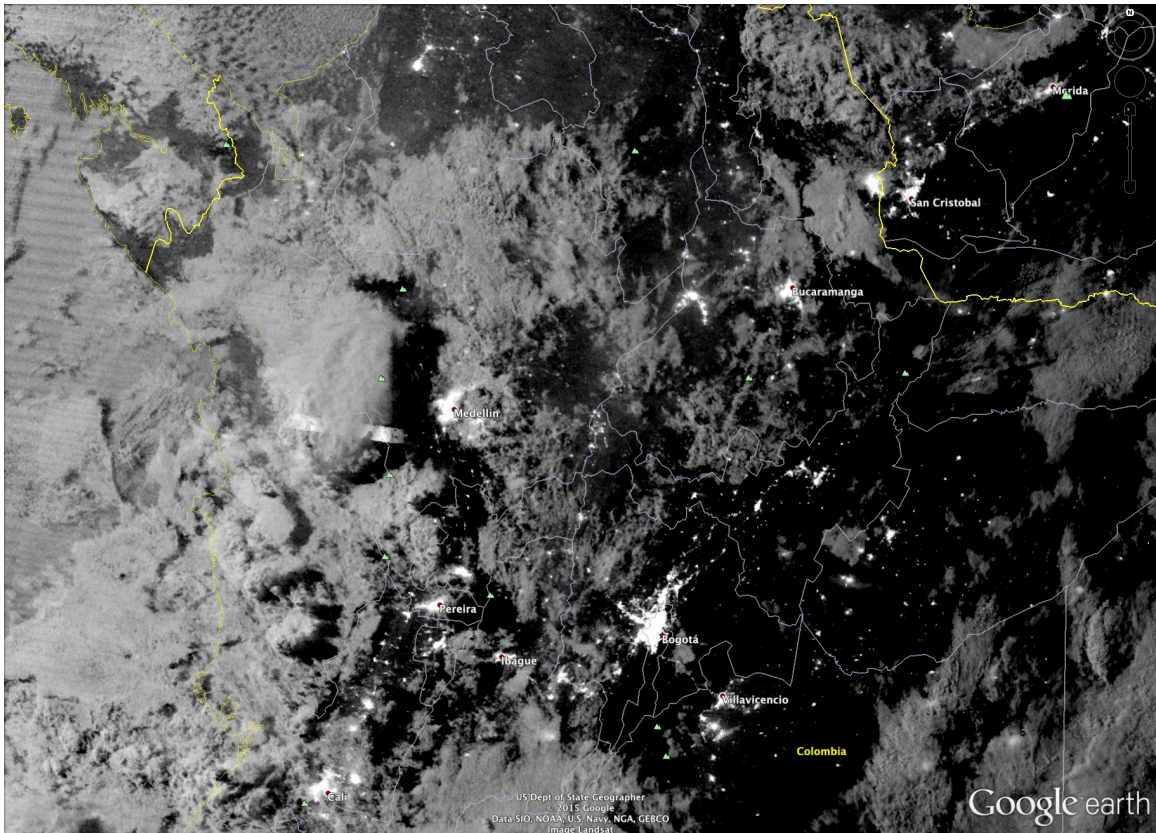


338



339

340 **Figure 6:** (top) Scatter plot of visible band M4 0.55  $\mu\text{m}$  reflectances (y-axis) against  
341 infrared window band M15 10.8  $\mu\text{m}$  brightness temperatures (x-axis). Pixels in the  
342 scatter plot are high-lighted in different colors and their locations are marked in the  
343 visible 0.55  $\mu\text{m}$  reflectance image (bottom). Purple highlights cold and reflecting cloud,  
344 green warm and non-reflecting land, and blue less-warm and non-reflecting ocean. The  
345 color mask can be clicked on and off with the check mark.



346

347

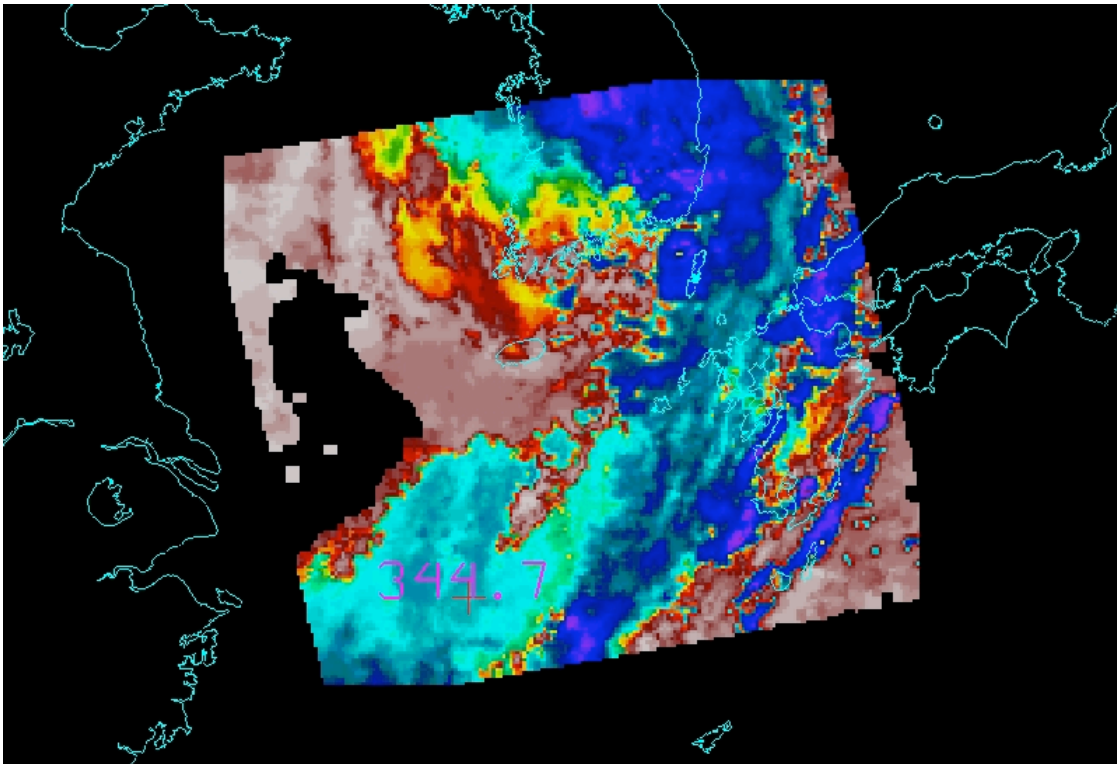
348 **Figure 7:** An example of a nighttime VIIRS visible image on 30 January 2015 over

349 Columbia, South America as displayed over Google Earth, as part of HYDRA2

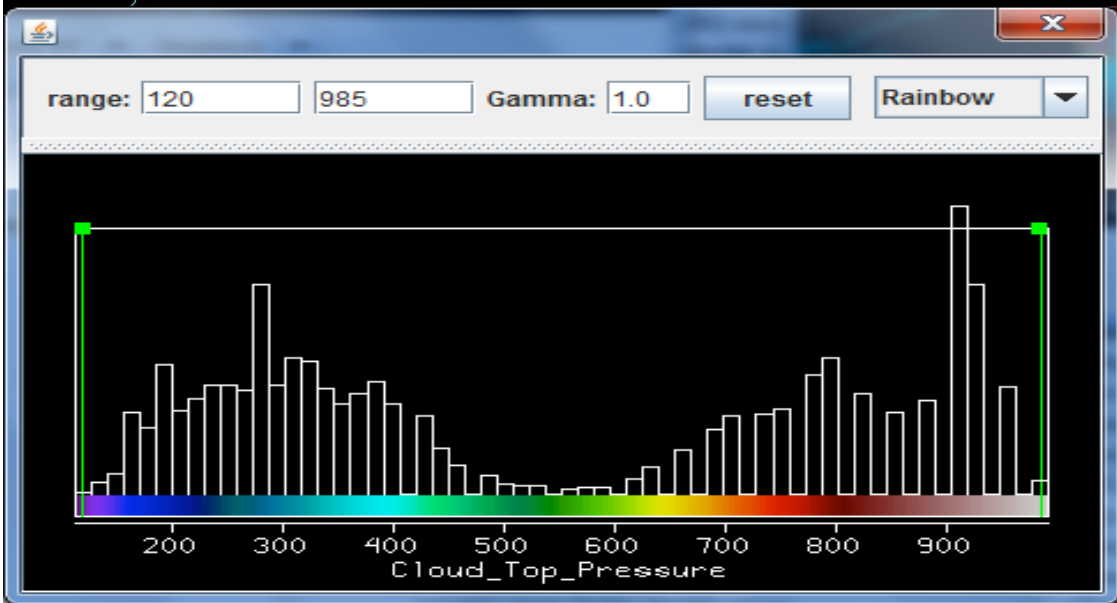
350 functionality.

351

352



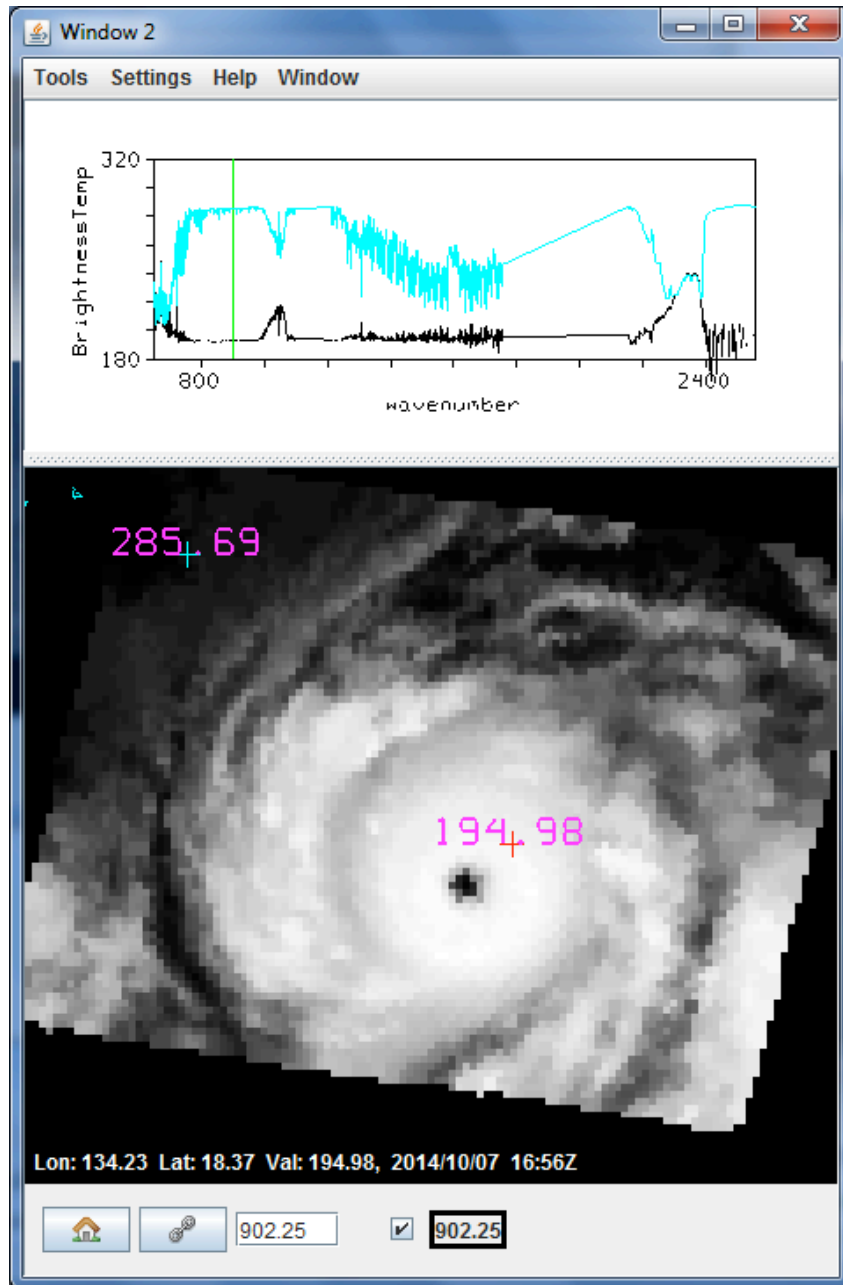
353



354

355

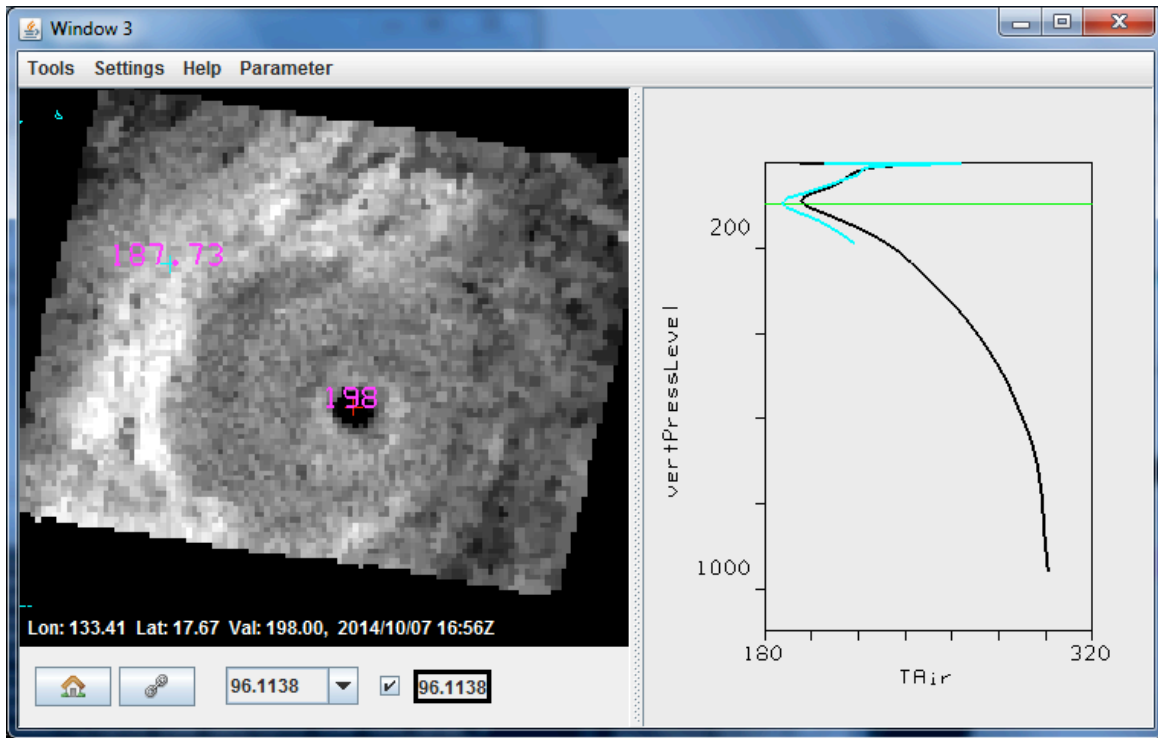
356 **Figure 8:** (Top) Derived image product of Aqua MODIS cloud top pressure levels (in  
 357 hPa) from the MODIS Level 2 (MOD06) cloud properties for 30 August 2012 at 440  
 358 UTC. (Bottom) Corresponding histogram and color code of cloud top pressure levels  
 359 within the entire image and associated color bar.



360

361

362 **Figure 9:** (bottom) Image of CrIS measurements (902 cm<sup>-1</sup> brightness temperatures in  
 363 degrees K ) over Typhoon Vongfong on 7 October 2012 indicating the locations of the  
 364 black spectrum (top) from clouds near the eye (marked by the red cross) and the  
 365 turquoise spectrum (top) from clear sky northwest of the typhoon (marked by the  
 366 turquoise cross).

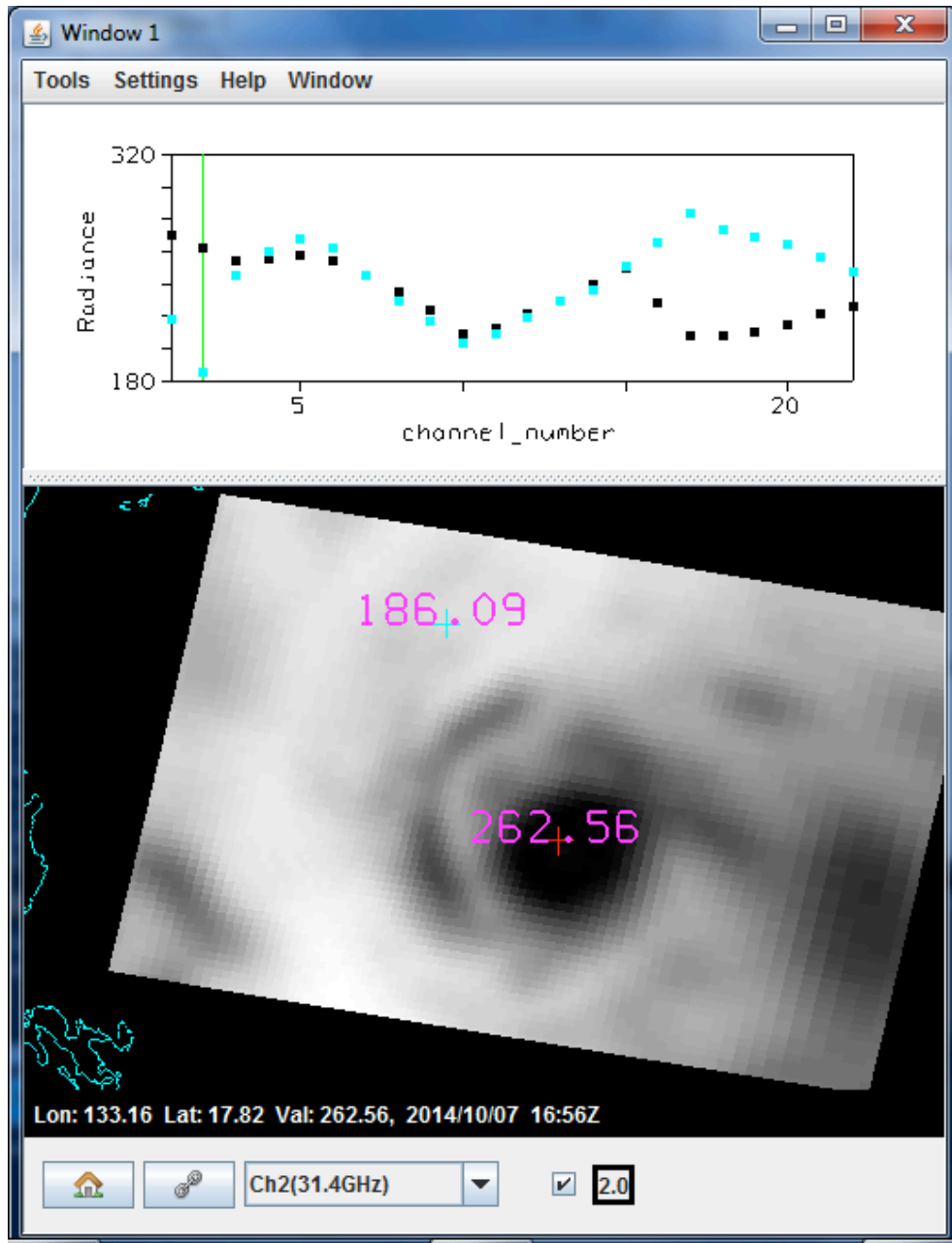


367

368

369 **Figure 10:** (left) Display of temperatures at 96.1 hPa over Typhoon Vongfong on 7  
 370 October 2012 using the Dual Regression Retrieval where white shades start at 185 K and  
 371 black shades start at 195 K. (right) Temperature profile retrievals down to cloud top in  
 372 the northwest sector of the typhoon (where the 96.1 hPa retrieved temperature is 187.73  
 373 K) is shown in black; the retrieval in the eye of the typhoon down to the ocean surface  
 374 (where the 96.1 hPa temperature is 198.0 K) is shown in turquoise. The green line  
 375 indicates the 96.1 hPa level.

376



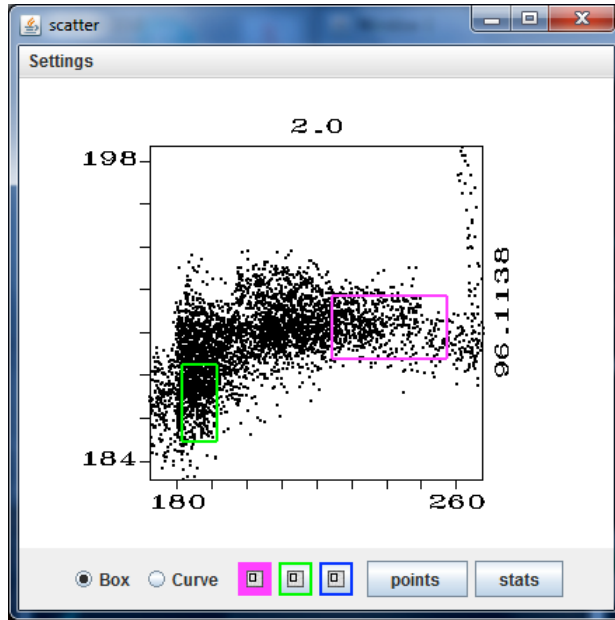
377

378

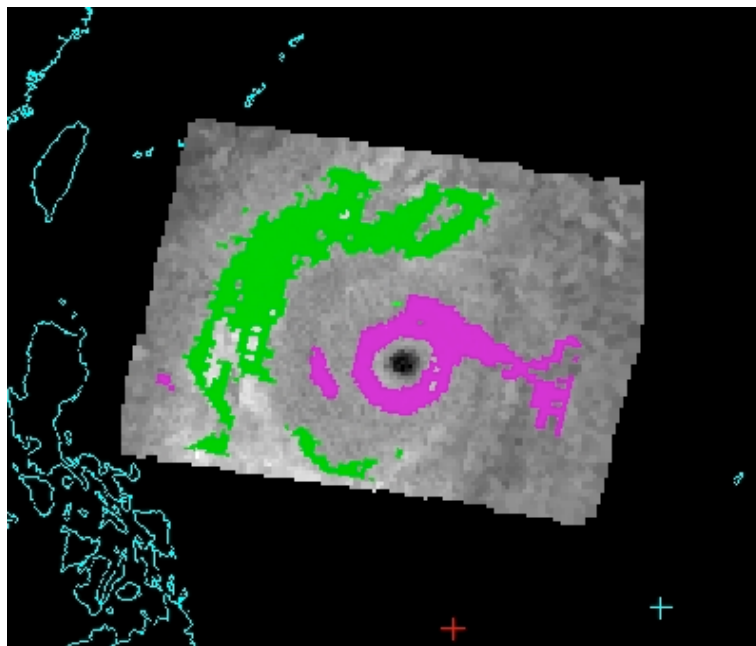
379 **Figure 11:** (Bottom) ATMS brightness temperature image for measurements over  
 380 Typhoon Vongfong on 7 October 2012 at 31.4 GHz (channel 2) along with (top)  
 381 microwave spectra from channel 1 at 23 GHz to channel 22 at 183.3 GHz in clouds  
 382 northwest of the typhoon center (turquoise dots) and in the eye (black dots).

383





384



385

386

387 **Figure 12:** (Top) Scatter plot of ATMS 31.4 GHz (Ch2) brightness temperatures on the  
 388 x-axis versus Dual Regression CrIS temperature retrievals at 96.1 hPa on the y-axis.

389 (Bottom) Green and purple pixels from scatter plot located in the 96.1 hPa temperature  
 390 image. All units are degrees Kelvin.

391

392 **Appendix 1. Getting and Setting Up HYDRA2**

393

394 The latest stable version of HYDRA2 can be obtaining from the following ftp site:

395

396 `ftp://ftp.ssec.wisc.edu/pub/CSPP/HYDRA2/`

397

398 For Windows Operating Systems (OS) (XP, VISTA 7 and 8) download the ‘exe’ file for  
399 latest version using binary ftp mode, and then run it by double-clicking the file icon. The  
400 installer will ask where you wish to install the program. Accept the default, C:\Program  
401 Files\HYDRA2. Start the program by selecting Start | All Programs | HYDRA2 |  
402 runHYDRA. A window named “HYDRA” will appear (Figure A1); it will indicate the  
403 version you are using. A window named “runHYDRA” will also appear (this window  
404 may be minimized, but do not close it).

405

406 For Mac OSX use the ‘dmg’ installer and simply double-click to install into the  
407 /Applications folder. To start HYDRA2, double-click the icon in that folder. The icon can  
408 also be dragged to the applications docking station after which a single click of the icon  
409 will start the application.

410

411 For the Linux OS (64bit), the ‘sh’ installer will extract into the directory of choice, or use  
412 the ‘tar.gz’ and install by entering “`gzip -cd hydra_v1.5_linux.tar.gz| tar xvf -`” at a  
413 command prompt. This will create a sub-directory named “hydra” into which everything  
414 required to run will be installed. To run HYDRA, first change directory into the 'hydra'  
415 directory, and enter “`./runHydra`” at the command prompt.

416

417 The HYDRA window enables you to load new files and to select regions within the  
418 current file. HYDRA is designed to read MODIS Level-1B 1KM files in HDF4 format.  
419 Files obtained from the NASA DAAC, or those produced locally by a direct broadcast  
420 ground station (including IMAPP), can also be used.

421

422

423

424 **Appendix 2. Summary of HYDRA 3.5 Commands**

425

426 *In all windows*

427

428 Shift-right click-drag to zoom in image within display

429

430 Right click-drag to move image or roam within display

431

432 *In HYDRA window (see Figure A1)*

433

434 Under File, select the VIIRS directory (a VIIRS folder) or File(s) (MOD02 or MYD02  
435 for MODIS, AIRS for AIRS, SCRIS for CrIS, SATMS for ATMS) that is to be studied.

436 (1) For VIIRS and MODIS, file selection will result in a listing of spectral bands  
437 available, an image of the IR window with coastlines, and a default subset of the granule  
438 that will be displayed in a new window upon clicking on display. The subset of the  
439 image can be adjusted with a right click and drag. The spectral band can be changed with  
440 a left click on another choice. (2) For CrIS, AIRS, and ATMS, a new window opens  
441 showing the spectral band brightness temperatures and a spectral window image showing  
442 the data coverage. Left click a drag on the green line in the top display to change the  
443 spectral band displayed below.

444

445 Left click on spectral band desired (default is IR window)

446

447 Left click-drag to highlight subset of image for display

448

449 Left click on Display at bottom to create a new image in window #1. Once Window#1 is  
450 established you can choose to replace the image in Window#1, to overlay a another  
451 image in Window#1, or to open a new Window#2 by using the arrows next to the Display  
452 command.

453

454 Tools/RGB Composite will open new a box where you have to select the R, G, and B  
455 spectral bands desired by left clicking on the color and then on the spectral band. When

456 all three have been selected, left click on Create in the RGB Composite window to  
457 establish the RGB image. Left click on Display in the main HYDRA window to open a  
458 new window wherein the RGB image is displayed.

459

460 Tools/Band Math will open a new display where you have to select two, three, or four  
461 spectral bands that you wish to combine with +, -, x, or / operations. Spectral bands are  
462 selected by left clicking on the spectral band and then the appropriate box in the Band  
463 Math equation. After selecting the desired Band Math click on create and the pseudo  
464 image dataset will appear under Combinations in the main HYDRA window. Click on  
465 Display to see the Band Math result in a new Window.

466

467 *In Window and Band Math Display (see Figure A2)*

468

469 Left click-drag to move cursor within display

470

471 Left click on bottom left icon (house) to restore original display

472

473 Left click on bottom box (indicating band number) to open range, gamma, reset, and  
474 B&W vs color options (see Figure A3)

475

476 Range can manually set BTmin (rmin) and BTmax (rmax). Range entries can be  
477 typed in to enhance low or high reflectances or BTs or they can be set by right  
478 click and sliding the top of the green bars in the reflectance/BT histogram. For the  
479 VIIRS DNB try very small values for your initial min to max range

480

481 Gamma can be adjusted to stretch the dynamic range. It is a non-linear mapping  
482 from color to value. For infrared,  $\text{color\_value} = \text{BT}^{**}\text{gamma}$ . For visible, when  
483  $\text{gamma} = 0.5$ , this is the square root enhancement popular with VIS.

484

485 Reset restores the dynamic range to the min and max values in the display.

486

487 Color options include inverse gray (BTmax is black, BTmin is white), gray,

488 rainbow (BTmax is red, BTmin is blue), and inverse rainbow. Contrast from  
489 white to black (or blue to red) can be adjusted in the range.

490

491 When overlays exist in a window, display can be moved from one overlay to another by  
492 clicking on the arrow at bottom of window. The check next to the band (or Band Math)  
493 identifier controls whether that image is contained in the loop controlled by the arrow at  
494 the bottom of the window. An overlay can be removed by clicking on the red circle to  
495 the right of the band identifier. (see Figure A4)

496

497 When two displays are open, toggle on link button in lower left to link zoom and roam in  
498 two displays (default is to have the windows linked)

499

500 After engaging Tools/Transect, one can left click-drag to change end point of the  
501 transect. Note that Transect can be opened in several windows simultaneously. (see  
502 Figure A5)

503

504 To engage Tools/Scatter, left click on Tools/Scatter in a first window to establish the x-  
505 axis and then left click on Tools/Scatter in a second window to establish the y-axis of  
506 scatter plot. The scatter plot will appear in a separate display. Two windows are  
507 necessary; Scatter is not properly initiated when using the overlay from one window  
508 alone.

509

510 Under Settings, options include coastlines (toggle for on and off), min/max display  
511 (toggle for on and off), probe readout (toggle for on and off for numerical value at cursor  
512 location), and color scale (toggle for on and off of numerical values associated with the  
513 colors in the display)

514

515 *In Scatter Display (see Figure A6)*

516

517 Selecting purple, green, and blue points (with box or curve) in the scatter window will  
518 show the associated pixels in the two image windows; conversely selecting pixels in  
519 either image window will show the associated points in the scatter window.

520

521 Left click on the points box (bottom of scatter window) to create density scatter plot;  
522 toggle back and forth between points and density

523

524 Left click on stats to see stats for purple, green, and blue selections.

525

526 Under Settings, Background Color allows selection of white or black background for the  
527 scatter plot and Axes allows resetting of x- and y-axes.

528

529 *In AIRS, CrIS, or ATMS SDR (Sensor Data Record) Display*

530

531 Select the file(s) to be displayed (AIRS for AIRS, SCRIS for CrIS, SATMS for ATMS)

532

533 Move the green line in the spectrum (left click drag) to change the spectral band  
534 displayed below.

535

536 When viewing the AIRS/CrIS/ATMS spectrum, zoom using shift- left click–drag.

537 Restore to full spectrum using control-left click.

538

539 When viewing AIRS/CrIS/ATMS spectral band image left click drag to move cursor  
540 within image (note if VIIRS data over same area is open then cursor will move in both  
541 VIIRS and CrIS/ATMS images; same for AIRS and MODIS)

542

543 Click on Tools to have the option for Transect, Scatter, and FourChannelCombine. In  
544 FourChannelCombine the colored lines have to be moved (left click drag) to the desired  
545 wavenumber (GHz). Expanding beyond two spectral bands is initiated by completing the  
546 mathematical operator desired in the FourChannelCombine equation.

547

548 When viewing AIRS or CrIS profile retrievals (temperature, water vapor, and ozone can  
549 be found under the parameter), transect and scatter (under Tools) can be used in the same  
550 way as before.

551

552 In the AIRS or CrIS Retrvl Display left click and drag on the green line in the vertical  
553 profile to change the altitude of the parameter being displayed.

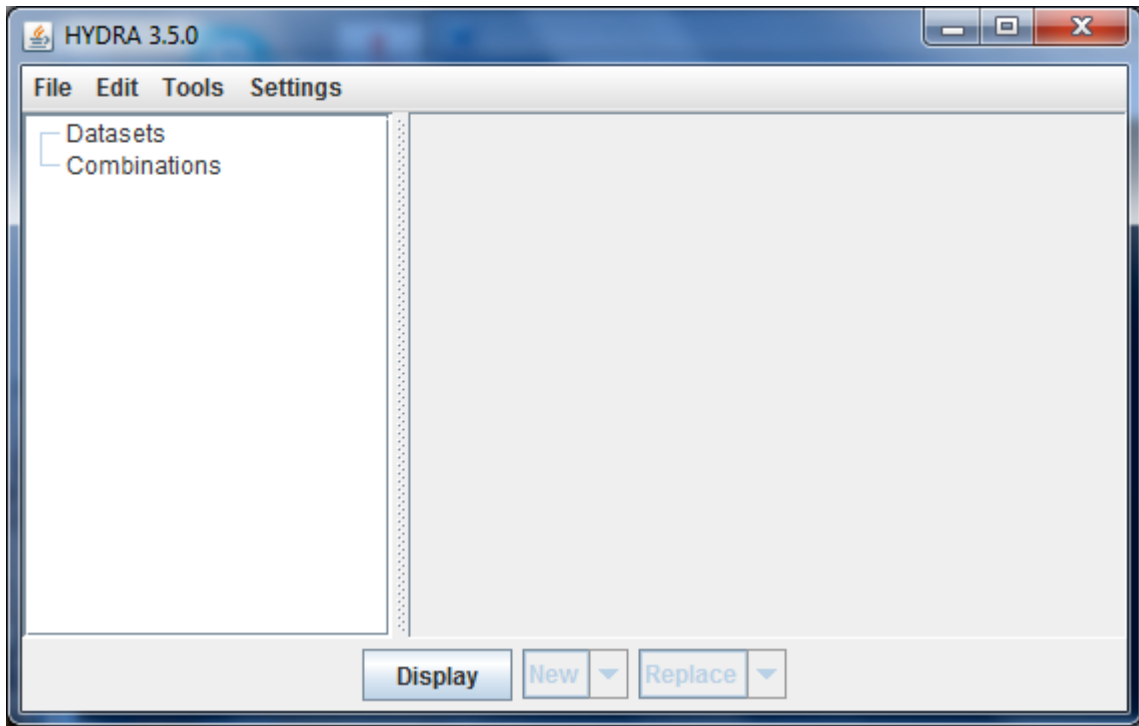
554

555 The red cursor in the CrIS Retrvl Display will move in synch with the red cursor in CrIS  
556 or VIIRS or ATMS spectral band displays; the blue cursor moves independent of any  
557 cursor in the other images.

558

559 Under Settings, in addition to the usual options, under Spectrum the background color  
560 can be switched from black or white.

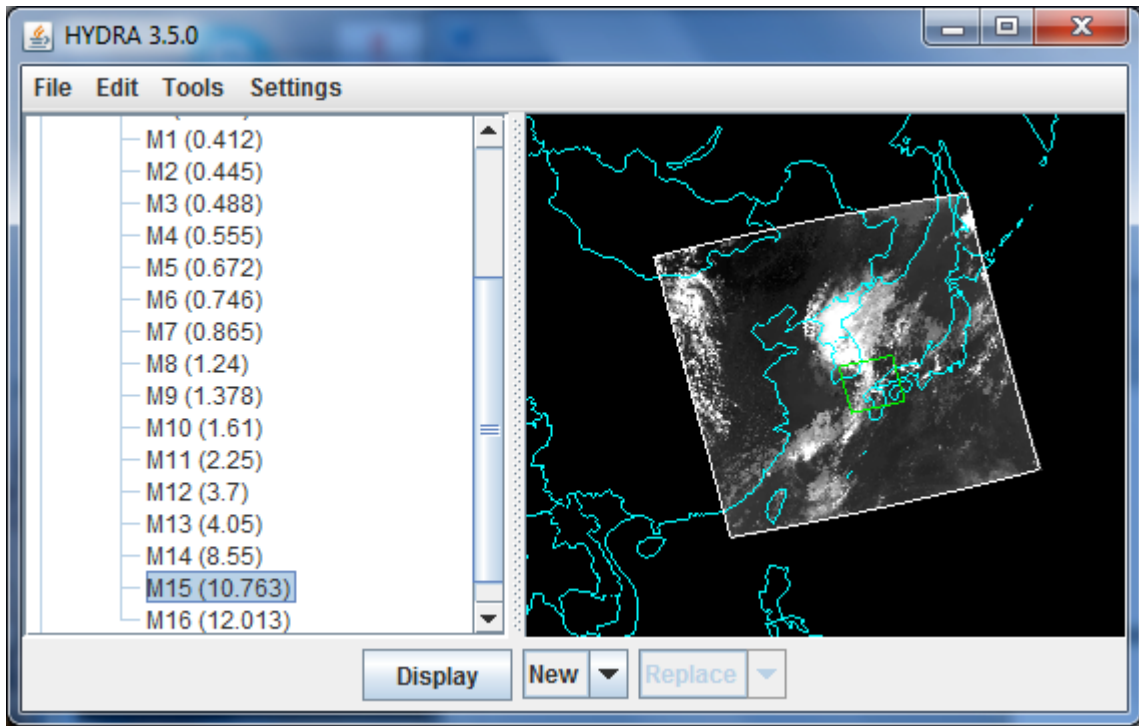
561



562  
563  
564  
565  
566

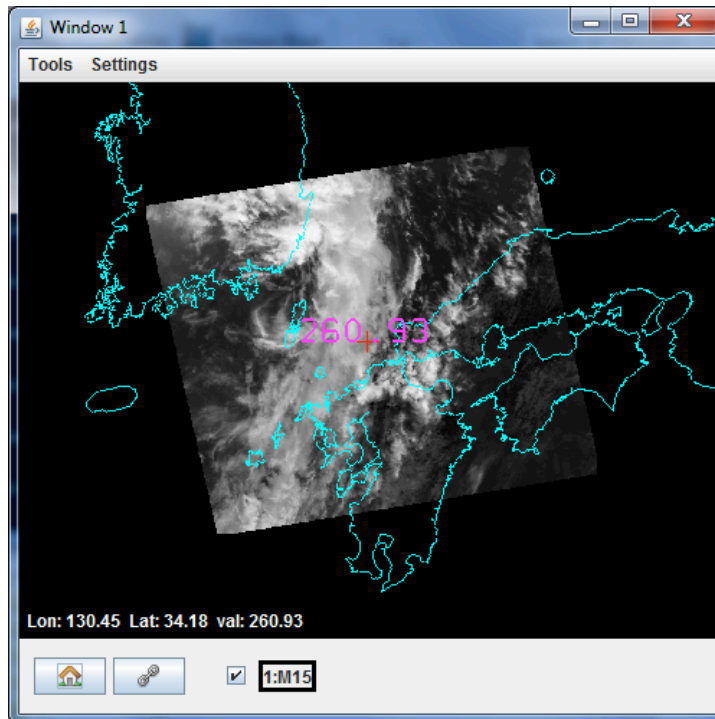
**Figure A1:** The HYDRA window before data set selection.



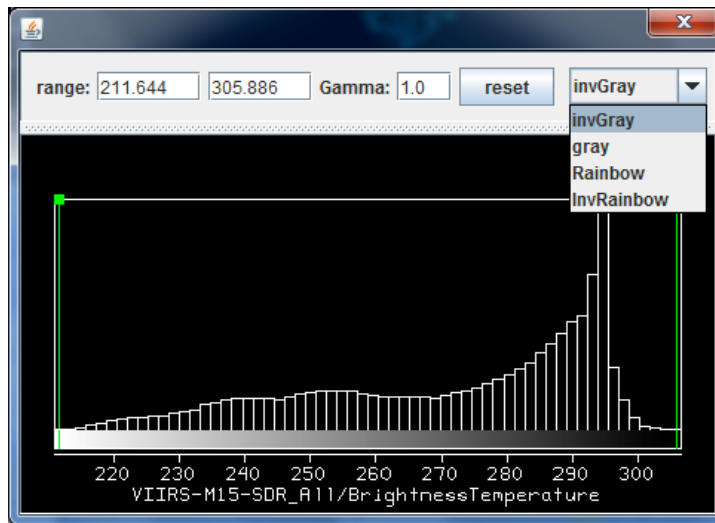


567  
568  
569  
570  
571

**Figure A2:** HYDRA window after selection of VIIRS data from 422 UTC on 30 August 2012 over Korea.



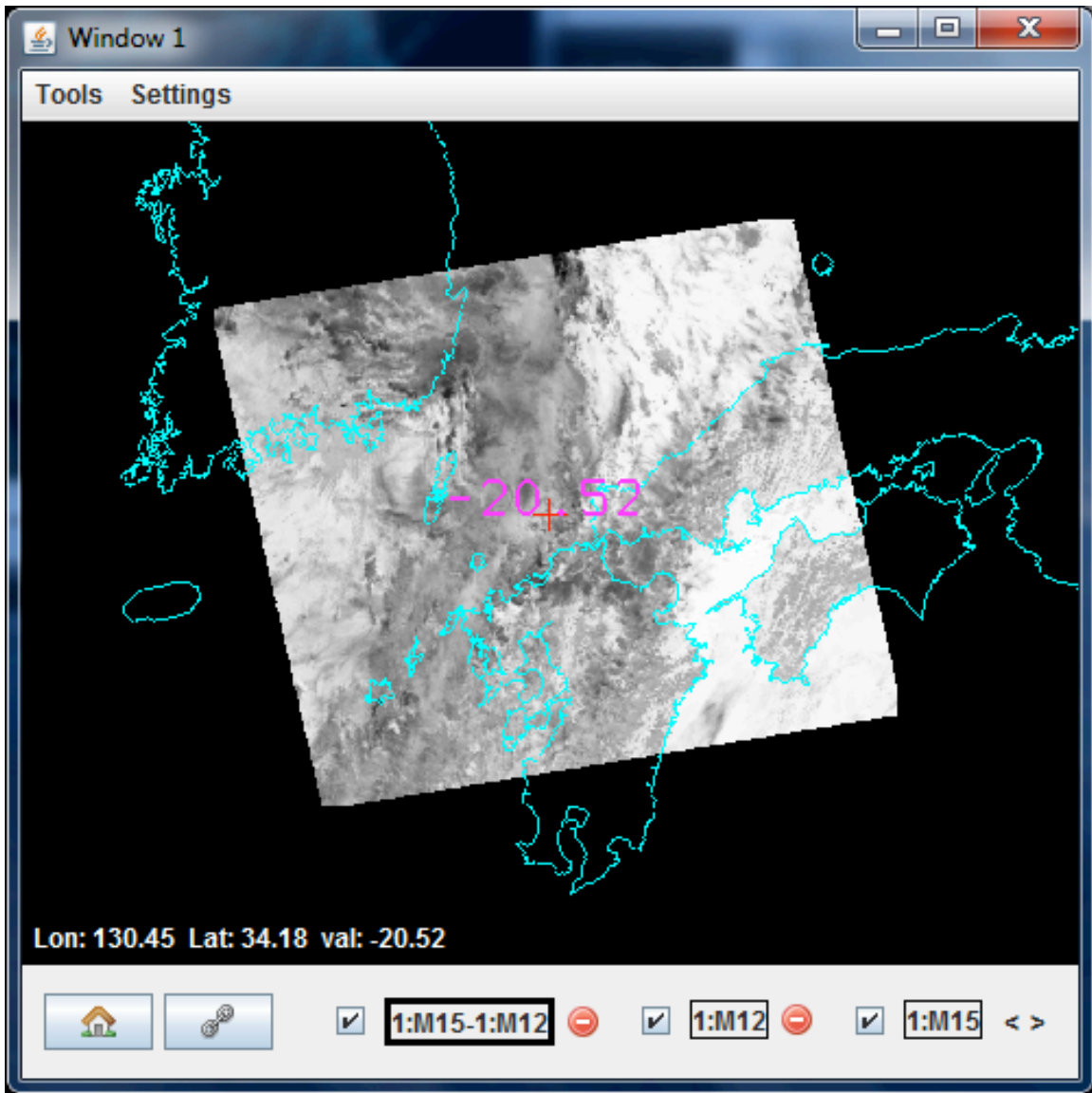
572



573

574

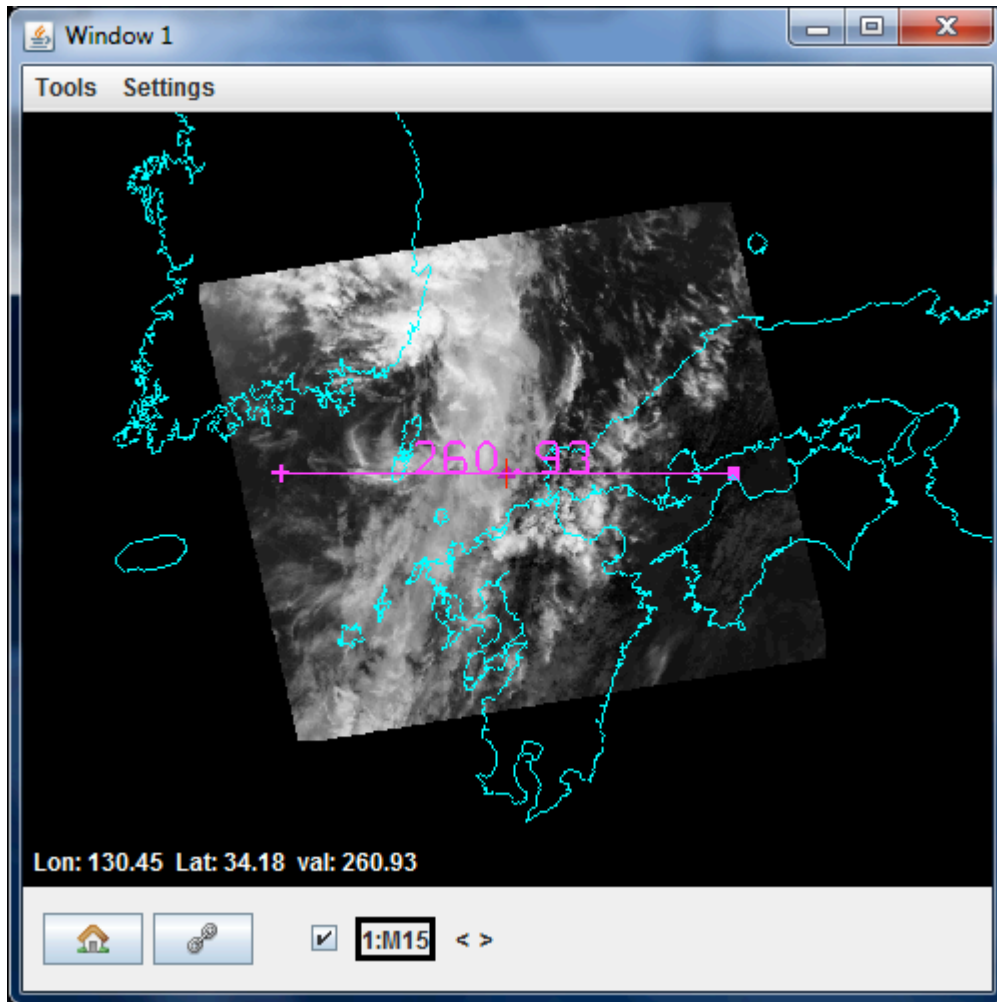
575 **Figure A3:** Image enhancement options opened by clicking on the box at the bottom of  
 576 the window indicating the spectral band. Range entries can be typed in to enhance low or  
 577 high reflectances or BTs or they can be set by right click drag on the top of the green bars  
 578 in the reflectance/BT histogram. Reset restores the dynamic range to the min and max  
 579 values in the display. Color options include inverse gray (BTmax is black, BTmin is  
 580 white), gray, rainbow (BTmax is red, BTmin is blue), and inverse rainbow.



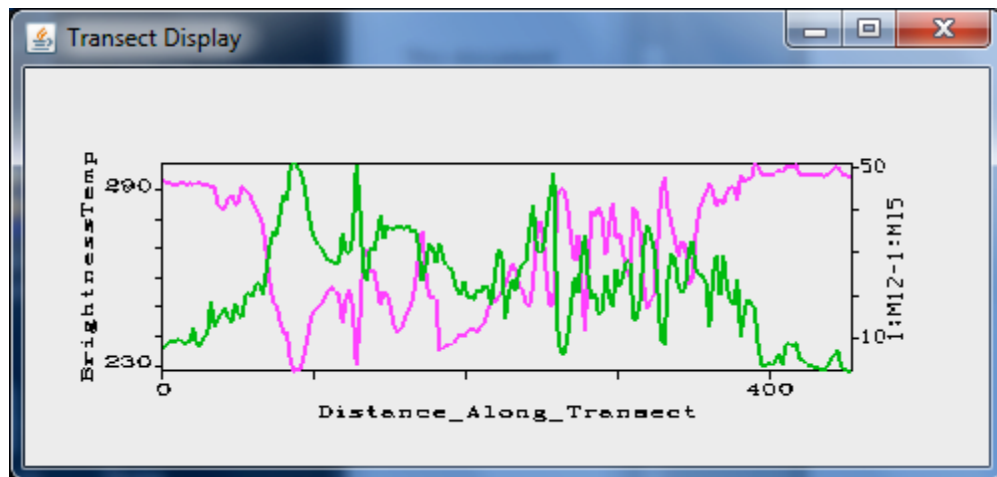
581

582

583 **Figure A4:** Window with overlay of three VIIRS brightness temperature images  
 584 (BT(M15) at 10.8  $\mu\text{m}$  minus BT(M12) at 3.7  $\mu\text{m}$ , BT(M12) at 3.7  $\mu\text{m}$ , and BT(M15) at  
 585 10.8  $\mu\text{m}$ ). The bold outline indicates which of the overlays is on display. When overlays  
 586 exist in a window, the display can be moved from one overlay to another by clicking on  
 587 the arrow at bottom right of the window. The check next to the band (or Band Math)  
 588 identifier controls whether that image is contained in the loop controlled by the arrow at  
 589 the bottom of the window. An overlay can be removed from the window by clicking on  
 590 the red circle to the right of the band identifier.



591



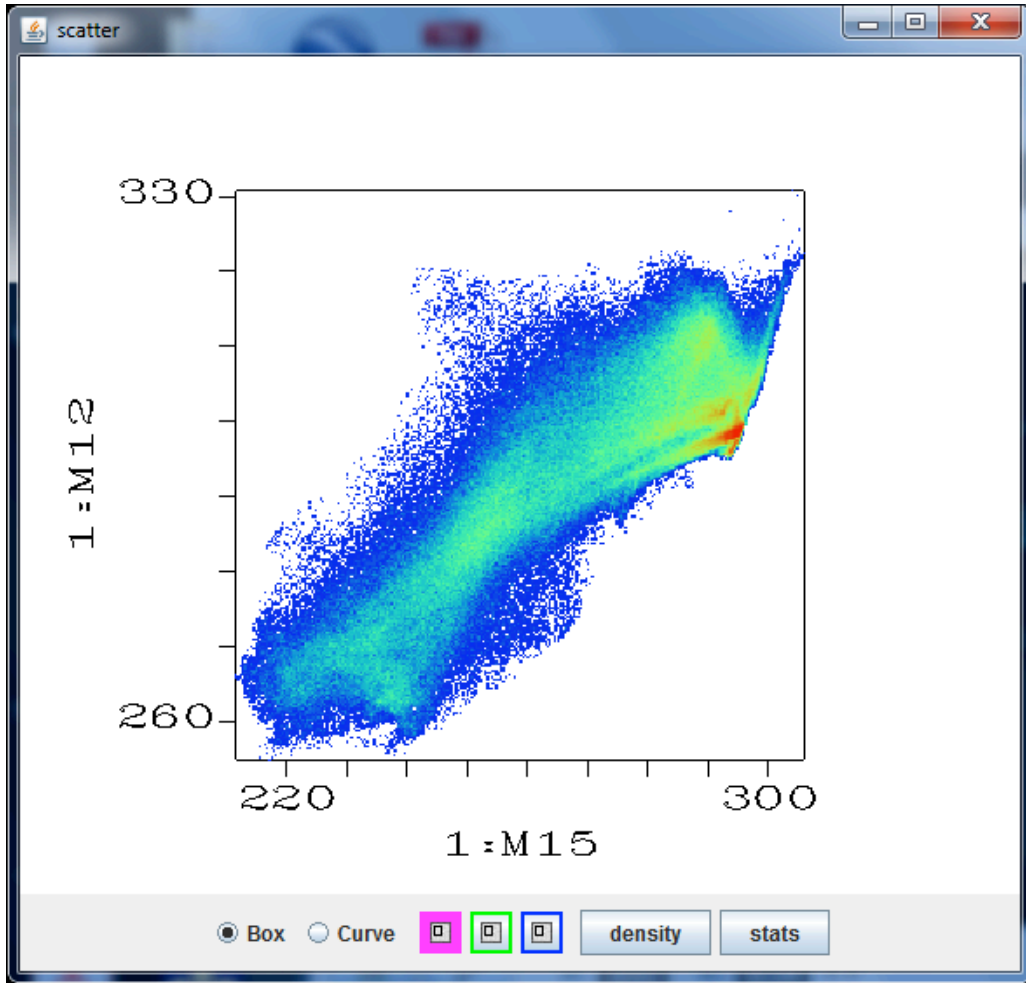
592

593

594 **Figure A5:** Transect Display of BT(M15) shown in the purple plot and [BT(M12)-

595 BT(M15)] shown in the green plot for M12 at 3.7  $\mu\text{m}$  and M15 at 10.8  $\mu\text{m}$ . The reflected

596 solar contributions often make BT(M12) greater than BT(M15).



597

Stats Parameter	NPP VIIRS 1:M15 2012/08/30 04:22Z	NPP VIIRS 1:M12 2012/08/30 04:22Z
Maximum	305.89	330.77
Minimum	211.64	254.83
Number of points	592620	592620
Mean	272.28	294.40
Median	279.88	298.07
Variance	475.31	173.39
Kurtosis	-0.71587	-0.06323
Std Dev	21.80	13.17
Correlation	0.84746	
Difference Maximum	-1.427	
Difference Minimum	-78.91	
Difference Mean	-22.11	
Area [km^2]		

598

599

600 **Figure A6:** (Top) Scatter window (in density mode) showing BT(M15 or 10.8  $\mu\text{m}$ ) on x-

601 axis versus BT(M12 or 3.7  $\mu\text{m}$ ) on y-axis. Red points show highest occurrence and blue

602 points show least. (Bottom) Scatter statistics for the pixels shown in the scatter plot.

603